http://dx.doi.org/10.5012/bkcs.2012.33.5.1613

Preparation of Ni Nanoparticles-TiO_2 Nanotube Arrays Composite and Its Application for Electrochemical Capacitor

Huichao He, Yunhuai Zhang, Peng Xiao,†,* Yannan Yang,‡ Qing Lou,† and Fei Yang

College of Chemistry and Chemical Engineering, Chongqing University, Chongqing 400030, PR China
*†College of Physics, Chongqing University, Chongqing 400030, PR China. *E-mail: xiaopeng@cqu.edu.cn*
‡Environmental Monitoring Station of Ziyang, Ziyang 641300, PR China
Received November 25, 2011, Accepted February 11, 2012

Ni nanoparticles-TiO_2 nanotube arrays (Ni/TiO_2NTs) composites were prepared by pulsed electrodeposition method and subsequently characterized by means of field emission scanning electron microscopy (FESEM), X-ray diffraction (XRD) and energy dispersive X-ray spectroscopy (EDX). The FESEM results showed that highly dispersed Ni nanoparticles were not only loaded on the top of the TiO_2NTs but also within the tubular structure, and the particle size of Ni prepared at different current amplitude (100, 200 and 300 mA·cm^{-2}) was in the range of 15 to 70 nm. The electrochemical studies indicated that Ni nanoparticles loaded on the highly ordered TiO_2NTs are readily accessible for electrochemical reactions, which improve the efficiency of the Ni nanoparticles and TiO_2NTs. A maximum specific capacitance (27.3 mF.cm^{-2}) was obtained on the Ni/TiO_2NTs composite electrode that prepared at a current of 200 mA.cm^{-2}, and the electrode also exhibited excellent electrochemical stability.

Key Words : Ni Nanoparticles, TiO_2 Nanotubes, Electrochemical capacitor

Introduction

Electrochemical capacitors (ECs), which combining the advantages of high power of dielectric capacitors and high energy density of second batteries, have attracted considerable attention for use in high power energy storage devices in recent years.[1-3] ECs can be classified by their reaction mechanisms into electrical double-layer capacitors (EDLCs) and pseudocapacitors. The EDLCs are based on non-faradic charge separation at the electrode/electrolyte interface, whereas the pseudocapacitors are based on the fast and reversible redox reactions at/near the surface of active materials. It is well known that pseudocapacitors show relatively less cycling stability than EDLCs because of the faradic reaction mechanism. However, pseudocapacitor electrodes show promise in asymmetric and/or hybrid configurations owing to their high specific capacitances and high volumetric capacitances as a result of the densely packed active materials. At present, carbon, conducting polymers and transition metal oxides are the most widely used active electrode materials.[4-7] Among these materials, amorphous hydrated RuO_2 exhibits the best properties thus far.[8] However, the high cost of RuO_2 has limited its commercial attractiveness for ECs applications and stimulated considerable effort on the search for alternative electrode materials.[9,10]

It has been reported that composite electrodes made from Ni nanoparticles and carbon nanotubes or TiO_2 nanotubes showed high specific capacitance and rate capability in alkali electrolyte duo to the increased surface area, electrochemical utilization of the active materials and ionic transport throughout the internal volume of the electrode.[11,12] Compared with the carbon nanotubes and TiO_2 nanotubes, highly ordered TiO_2 nanotube arrays (TiO_2NTs) formed on Ti substrate not only offer the direct path for electrons toward the current collector, but also with lower fabrication cost and higher accessible surface for electrochemical reactions. In addition, its large surface areas, high packing densities and ordered pore networks are expected to facilitate rapid charge/discharge kinetics.[13,14] Consequently, TiO_2NTs used as a support to load highly dispersed Ni nanoparticles will possess enhanced capacitance because such composite structure can provide more readily available spaces for electrochemical reactions.

In this study, Ni nanoparticles-TiO_2NTs composites were by pulsed electrodeposition method and employed as functional electrode materials. The electrochemical properties of the Ni/TiO_2NTs as pseudocapacitor electrodes were investigated by a series of electrochemical tests.

Experimental

Preparation of Ni/TiO_2NTs Composite Electrode. TiO_2NTs were prepared by anodization method.[15] Ti foils were degreased by sonicating in acetone and methanol, rinsed with deionized water and dried in nitrogen stream. The samples were anodized in 0.15 mol·L^{-1} HF electrolyte with a platinum foil as a counter electrode at 20 V for 2 hrs. And then the as-anodized TiO_2NTs were annealed in nitrogen atmosphere at 400 °C for 3 hrs to convert the amorphous TiO_2NTs to the crystalline form. Ni nanoparticles were loaded on the as-annealed TiO_2NTs by pulsed electrodeposition method.[16] Deposition experiments were performed in three-electrode system with nickel plate as a counter

electrode and Ag/AgCl electrode as a reference electrode. The deposition bath was a mixture of 300 g·L^{-1} $NiSO_4·6H_2O$, 45 g·L^{-1} $NiCl_2·6H_2O$, 37 g·L^{-1} H_3BO_3, pH=4.4. The electrolyte temperature was kept at 38 °C. The Ni/TiO_2NTs composites were prepared at constant current off-time (1000 ms), pulse time of both negative and positive current (8 ms, 2 ms) and different current amplitudes: 100, 200 and 300 mA.cm^{-2}. Total charge density was fixed at 0.623 C.cm^{-2}.

Measurements. Morphological characterization was carried out by field emission-scanning electron microscope (FESEM; Nova 400 Nano-SEM). Crystalline structure of the samples was examined by an X-ray diffraction (XRD) with Cu Kα radiation. The content of Ni was identified by an energy dispersive X-ray spectroscopy (EDX; INCA Energy 350).

All electrochemical measurements were carried out in a three-electrode system with a 1.0 mol·L^{-1} NaOH solution. The as-prepared samples with a geometric area of 1.0 cm^2 were placed as the working electrode, a platinum foil as a counter electrode and a saturated calomel electrode (SCE) as reference electrode. Electrochemical impedance spectroscopy (EIS) measurement was performed by Autolab PGSAT32/FRA impedance system. CHI600C electrochemical workstation (Shanghai, China) was employed for the cyclic voltammetry (CV) and chronopotentiometric (CP) tests.

Results and Discussion

Morphology and Crystallization Characterization. Figure 1(a) shows the FESEM image of TiO_2NTs before deposition of Ni nanoparticles. The average interior diameter and tube length of TiO_2NTs were about 100 and 400 nm, respectively, which were advantageous for the ingress of Ni^{2+} and deposition of Ni nanoparticles inside nanotubes. Figure 1(b), 1(c) and 1(d) present the FESEM images of Ni/TiO_2NTs prepared at 100, 200 and 300 mA.cm^{-2}, respectively. It can be observed that dispersed Ni nanoparticles were loaded uniformly on the top of TiO_2NTs. In addition, some relatively small Ni nanoparticles were observed present into the tubes (inset in Figure 1(c)). Ni/TiO_2NTs with such architecture can provide abundant sites for reversible redox reaction. The particle size of Ni deposited at 100, 200 and 300 mA.cm^{-2} is about 70, 15 and 40 nm, respectively. The reduction in particle size with the increase of current amplitudes is due to the higher overpotential and the accompanying increase in nucleation rate.[17] However, when the deposition current increased to 300 mA.cm^{-2}, the percentage of current for the reduction of H^+ increased, leading to lower efficiency for nickel deposition. That is, nucleation rate of nickel decreased greatly, resulting in an increase of particle size from 15 to 40 nm (Figure 1(d)), which is consistent with the findings of Yoshimura.[18]

Figure 2 shows XRD patterns of the annealed TiO_2NTs and Ni/TiO_2NTs composites. In the XRD pattern of TiO_2NTs, an anatase characteristic diffraction peak (2θ = 25.3°) was showed evidently. But after nickel deposition, two new characteristic peaks located at 2θ = 44.5° and 51.8° corresponding to Ni (111) and (200), respectively, which is in agreement with previous data reported by Wang's group.[19] These results confirmed that Ni particles were deposited onto the TiO_2NTs and the composite was Ni/TiO_2NTs.

EDX measurement was carried out to determine the elemental composition in Ni/TiO_2NTs composites. The loading amounts of Ni deposited at 100, 200 and 300 mA.cm^{-2} were 9.51, 16.37 and 11.02 at% (atomic percentage), respectively. At the highest current (300 mA.cm^{-2}), hydrogen evolution occurred at a high rate, which decreased current electrodeposition and destroyed the surface of Ni/TiO_2NTs electrode. As a result, the Ni loading amounts decreased from 16.37 to 11.02 at%.

Electrochemical Properties. Figure 3 shows cyclic voltammograms of the as-annealed TiO_2NTs and Ni/TiO_2NTs electrodes prepared at 100, 200 and 300 mA.cm^{-2}. It is obvious that TiO_2NTs shows low current response, which indicates small specific capacitance. For Ni/TiO_2NTs, higher current responses were observed, which suggest the pseudocapacitance is mainly come from Ni nanoparticles on Ni/TiO_2NTs composites. In the anodic scan, non-faradic

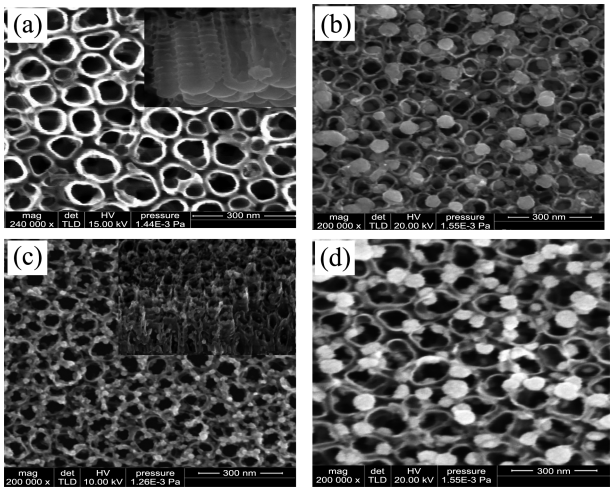

Figure 1. FESEM images of (a) TiO_2NTs and Ni/TiO_2NTs prepared at (b) 100, (c) 200 and (d) 300 mA.cm^{-2}.

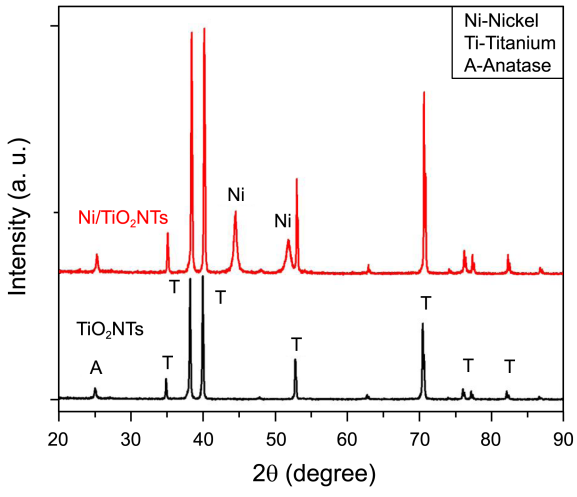

Figure 2. X-ray diffraction patterns of TiO_2NTs and Ni/TiO_2NTs.

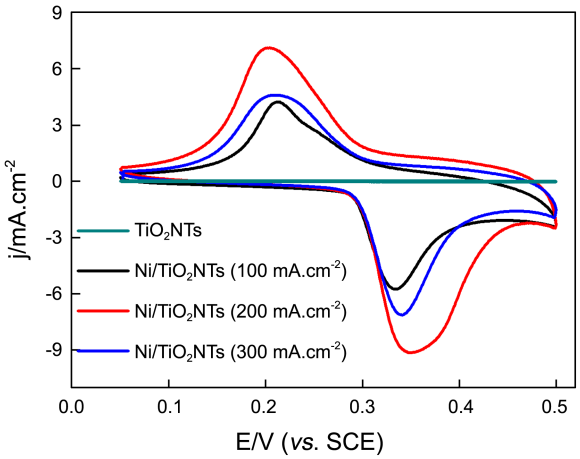

Figure 3. Cyclic voltammograms of TiO_2NTs and Ni/TiO_2NTs prepared at different current amplitude in 1 M NaOH at potential sweep rates of 100 mV.s^{-1}.

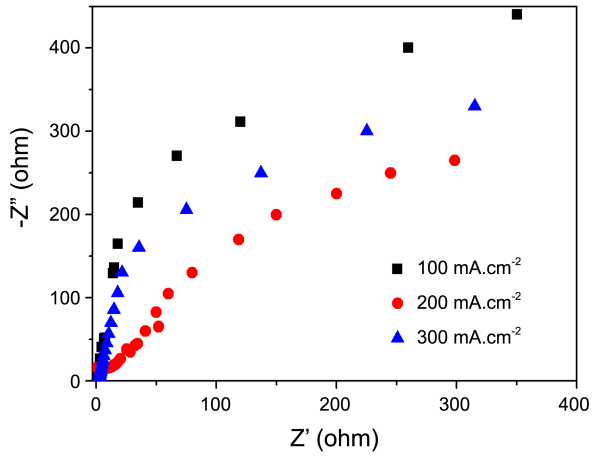

Figure 4. Electrochemical impedance spectroscopy of Ni/TiO_2NTs prepared at different current amplitude in 1 M NaOH.

adsorption of OH^- and possible double-layer charging process would occur at the initial stage from 0 to 0.29 V.[20] Then, owing to the appearance of the redox peak pair, faradic reactions have occurred to cause a good performance of faradic capacitance. This capacitance characteristic of Ni/TiO_2NTs was distinct from that of the electric double-layer capacitor, which would produce a CV curve close to an ideal rectangular shape.[3,21] Herein the measured capacitance was mainly based on the reversible redox reaction mechanism due to the quasi-reversible electron transfer process. A broad oxidation peak appeared at about 0.34 V was ascribed to the oxidation of both the Ni deposited to $Ni(OH)_2$ and the newly formed $Ni(OH)_2$ to NiOOH. A reduction peak was observed at about 0.21 V, which was associated with the reduction of the NiOOH back to $Ni(OH)_2$. This reversible redox reaction was written schematically as follows[22,23]:

$$Ni(OH)_2 + OH^- \Leftrightarrow NiOOH + H_2O + e^- \quad (1)$$

As shown in Figure 3, the CV current density of Ni/TiO_2NTs increased with the increase of the deposition current amplitude and reached a maximum when the deposition current was 200 mA.cm^{-2}. It can be explained by taking into account that the amount of Ni deposited at this current is at maximum value (16.37 at%) and the Ni particle size (15 nm) is the smallest, which would provide most abundant active sites for reversible redox reactions. The highest current density indicates that the Ni/TiO_2NTs composite electrode prepared at 200 mA.cm^{-2} possess a highest specific capacitance than that of 100 and 300 mA.cm^{-2}.

Figure 4 presents the impedance spectra in the form of Nyquist plots for the Ni/TiO_2NTs composite electrodes measured at 0 V. As shown in Figure 4, the depressed semicircles appeared within the entire frequency range in Nyquist impedance plots, which indicated the composite electrodes predominantly conducted a kinetics-controlled electrochemical process, and the impedance was mainly determined by the charge-transfer resistance at the interface of electrolyte/active material/current collector. Regarding three designated Ni/TiO_2NTs electrodes, the difference of impedance curves at high frequencies was mainly attributed to the limitation degree of the interfacial charge transfer between Ni/TiO_2NTs composite and the electrolyte. Corresponding resistance of these electrodes could be qualitatively estimated by comparing the diameter of the semicircle-like arc at high frequencies. Impedance analysis shows the diameter of the Nyquist plot on the Ni/TiO_2NTs composite electrode prepared at 200 mA.cm^{-2} is the smallest, which indicates that the electrode has minimum charge-transfer resistance. It can be attributed to: (1) The maximum amount of electroactive Ni loading on TiO_2NTs resulted in the composite electrode possesses a highest electrical conductivity; (2) Smallest Ni nanoparticles obtained at 200 mA.cm^{-2} could provide maximum electrochemically active surface area, which decreased the charge-transfer resistance at the interface.

Electrochemical Capacitance. Figure 5(a) shows the charge-discharge curves of Ni/TiO_2NTs composite electrodes at a current density of 0.1 mA.cm^{-2} in a potential window (0 to 0.45 V). The charge process mostly occurred at a potential above 0.34 V till to the designated potential due to the oxidation of both Ni to $Ni(OH)_2$ and then $Ni(OH)_2$ to NiOOH, which was in good agreement with the results of the CV curve. The discharge process exhibited a plateau around 0.24 to 0.31 V, corresponding to the reduction of the NiOOH back to $Ni(OH)_2$. The specific capacitances of Ni/TiO_2NTs composite electrodes synthesized at different current amplitudes were calculated according to the following Equation:

$$C_S = \frac{C}{S} = \frac{I \times t}{\Delta V \times S} \quad (2)$$

Where I is charge-discharge current; t, discharge time; ΔV, potential change; and S is the apparent surface area of Ni/TiO_2NTs electrode.[24] The results show the specific capacitances of the composite electrodes prepared at 100, 200 and 300 mA.cm^{-2} is 5.8, 27.3 and 15.1 mF.cm^{-2}, respectively. Obviously, the composite electrode prepared at 200 mA.cm^{-2} has maximum specific capacitance, which can be explained by taking into account that:

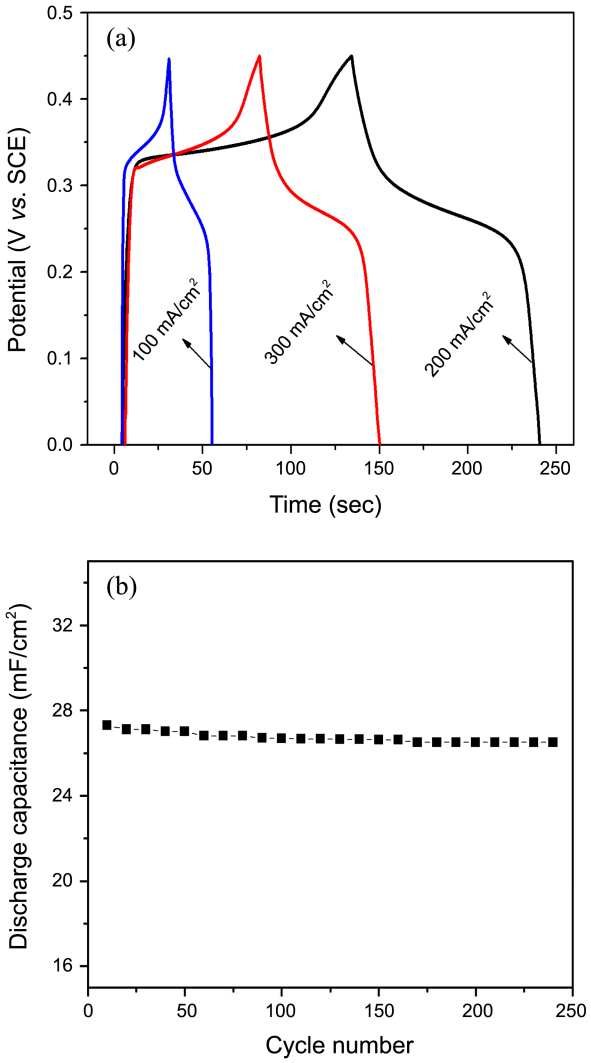

Figure 5. (a) The charge-discharge curves of Ni/TiO_2NTs composite electrodes at a current density of 0.1 mA.cm^{-2} within a potential window (0 to 0.45 V *vs*. SCE). (b) Chronopotentiometric curve of the Ni/TiO_2NTs composite electrode prepared at 200 mA.cm^{-2}.

(1) The Ni nanoparticles with a largest electrochemically active surface area can provide more accessible spaces for the electrolyte, resulting in more feasible electro-redox reaction at the interface of nickel and alkali electrolyte in the charge-discharge process; (2) The maximum amount of electroactive Ni loading on TiO_2NTs can form abundant active sites and decrease the charge-transfer resistance at the interface. The electrochemical stability of the Ni/TiO_2NTs composite electrode prepared at 200 mA.cm^{-2} has been further examined by chronopotentiometry. As shown in Figure 5(b), the specific capacitance loss after 250 cycles was about 5%, indicating excellent electrochemical stability.

Conclusions

In summary, Ni nanoparticle-TiO_2 nanotube arrays composite electrodes were prepared by pulsed electrodeposition method and constructed for electrochemical capacitor application. It was found that the Ni/TiO_2NTs composite electrode prepared at 200 mA.cm^{-2} had maximum specific capacitance (27.3 mF.cm^{-2}) and excellent cycle stability due to the smallest Ni nanoparticle loaded on TiO_2NTs offers highest active surface area for electro-redox reaction. The present study shows Ni/TiO_2NTs can act as a promising candidate for the electrochemical capacitor application.

Acknowledgments. This work was supported by the Postgraduate Science and Innovation Fund of Chongqing University (Grant No. 200904A1A0010310), Natural Science Foundation Project of CQCSTC, 2009BB4047 and Innovative Talent Training Project, the Third Stage of "211 project", Chongqing University (Grant No. S-09103).

References

1. Prasad, K. R.; Miura, N. *Electrochem. Commun.* **2004**, *6*, 1004.
2. Cao, L.; Xu, F.; Liang, Y. Y.; Li, H. L. *Adv. Mater.* **2004**, *16*, 1853.
3. Wang, Y. G.; Li, H. Q.; Xia, Y. Y. *Adv. Mater.* **2006**, *18*, 2619.
4. Conway, B. E. *Electrochemical Supercapacitors*; Scientic Fundamentals and Technological Applications, Kluwer Academic/Plenum Publishers: New York, 1999.
5. Frackowiak, E. *Phys. Chem. Chem. Phys.* **2007**, *9*, 1774.
6. Subramanian,V.; Zhu, H. W.; Vajtai, R.; Ajayan, P. M.; Wei, B. Q. *J. Phys. Chem. B* **2005**, *109*, 20207.
7. Wang, Y. G.; Xia, Y. Y. *Electrochim. Acta* **2006**, *51*, 3223.
8. Sugimoto, W.; Iwata, H.; Yasunaga, Y.; Murakami, Y.; Takasu, Y. *Angew. Chem. Int. Ed.* **2003**, *42*, 4092.
9. Koysuren, O.; Du, C.; Pan, N.; Bayram, G. J. *Appl. Polym. Sci.* **2009**, *113*, 1070.
10. Nam, K. W.; Kim, K. H.; Lee, E. S.; Yoon, W. S.; Yang, X. Q.; Kim, K. B. *J. Power Sources* **2008**, *182*, 642.
11. He, K. X.; Zhang, X. G.; Li, J. *Electrochim. Acta* **2006**, *51*, 1289.
12. Hsieh, C. T.; Chou, Y. W.; Chen, W. Y. *J. Solid State Electrochem.* **2008**, *12*, 663.
13. Wang, D. W.; Fang, H. T.; Li, F.; Chen, Z. G.; Zhong, Q. S.; Lu, G. Q.; Cheng, H. M. *Adv. Funct. Mater.* **2008**, *18*, 3787.
14. Ortiz, G. F.; Hanzu, I.; Djenizian, T.; Lavela, P.; Tirado, J. L.; Knauth, P. *Chem. Mater.* **2009**, *21*, 63.
15. Gong, D.; Grimes, C. A.; Varghese, O. K.; Hu, W.; Singh, R. S.; Chen, Z.; Dickey, E. C. *J. Mater. Res.* **2001**, *16*, 3331.
16. Zhang, Y. H.; Yang, Y. N.; Xiao, P.; Zhang, X. N.; Lu, L.; Li, L. *Mater. Lett.* **2009**, *63*, 2429.
17. Puippe, J. C.; Ibl, N. J. *Appl. Electrochem.* **1980**, *10*, 775.
18. Yoshimura, S.; Chida, S.; Sato, E.; Kubota, N. *Metal Finish.* **1986**, *84*, 39.
19. Wang, H. Z.; Kou, X. L.; Zhang, L.; Li, J. G. *Mater. Res. Bull.* **2008**, *43*, 3529.
20. Kalu, E. E.; Nwoga, T. T.; Srinivasan, V.; Weidner, J. W. *J. Power Sources* **2001**, *92*, 163.
21. Frackowiak, E.; Beguin, F. *Carbon* **2001**, *39*, 937.
22. Tai, Y. L.; Teng, H. *Carbon* **2004**, *42*, 2329.
23. Ragan, D. D.; Svedlindh, P.; Granqvist, C. G. *Sol. Energy Mater. Sol. Cells* **1998**, *54*, 247.
24. Wang, Y. G.; Zhang, X. G. *J. Electrochem. Soc.* **2005**, *152*, A671.